

# **Power control of LCR-DAB converter with phase shift in fixed switching frequency**

Seung-Hyuk Baek<sup>1</sup>, Jaehong Lee<sup>2</sup>, Seung-Hwan Lee<sup>2</sup>, and Sungmin Kim<sup>3</sup>

<sup>1</sup>Power ICT Research Center, Korea Electrotechnology Research Institute  
Ansan, South Korea

<sup>2</sup>School of Electrical and Computer Engineering, University of Seoul  
Seoul, South Korea

<sup>3</sup>Department of Electrical and Electronic Engineering, Hanyang University  
Ansan, South Korea

Tel.: +82 / (031) 8040-4270  
E-Mail: seunghb@keri.re.kr

## **Keywords**

«Dual Active Bridge Converter», «DC-DC power converter», «Bi-directional converters», «Solid-State Transformer», «Wireless Power Transmission»

## **Abstract**

This paper proposes the power control method of the Loosely Coupled Resonant Dual-Active-Bridge (LCR-DAB) converter using Phase-Shift Modulation (PSM) of a conventional DAB converter. In this paper, to apply PSM to the LCR-DAB converter, the impedance characteristics were analyzed to design an efficient operating frequency for the LCR-DAB converter. In addition, the power equation of the LCR-DAB converter was derived to control the power using the phase, which is the control variable of the PSM. Experiments were performed on the 840W prototype LCR-DAB converter to verify the validity of the proposed power control method.

## **Introduction**

According to the increase of grid-connected distributed energy resources, the need for large-capacity power conversion systems is being emphasized. To increase the power density of a high-power converter, research on a Solid-State Transformer (SST) that converts power through converters with high-frequency transformers instead of line frequency transformers is being actively conducted [1-7]. Since the insulation performance of the SST is determined by the high-frequency transformer of the Dual-Active-Bridge (DAB) converter in the SST, the design of the high-frequency transformer has been becoming very important. To achieve the high-power density of SST, the size of the high-frequency transformer needs to be as small as possible. However, the high voltage insulation of the transformer requires enough volume of the transformer. To solve this problem, the Loosely Coupled Resonant DAB (LCR-DAB) converter using Wireless Power Transfer (WPT) coils with a low coupling coefficient instead of the high-frequency transformer was studied [8-9]. The LCR-DAB converter can secure high insulation performance because there is a physical gap between the two WPT coils. And, to enhance the efficiency of the power transfer, the series capacitors are employed with the WPT primary and secondary coils, respectively. In this paper, the impedance characteristics of the WPT coil and the series capacitor has been analyzed and the power transferred between two active bridge converters have been derived according to the output voltage of the two converters. Based on the impedance characteristics and the transferred power, the simple power control method of the LCR-DAB converter is newly presented in this paper. The proposed power control method uses the fixed frequency Phase-Shift Modulation (PSM), which is the power control method of the conventional Dual-Active-Bridge (DAB) converter having only a high-frequency transformer. The PSM based fixed frequency power control method can determine the transferred power between primary and secondary power by the phase angle difference of the primary and secondary output voltage. Since the proposed method uses only a single parameter, phase angle difference, the power control can be simply implemented. In this paper, the frequency characteristics for selecting the

operating frequency of the LCR-DAB converter are explained, and the validity of the proposal is verified through the power control experiment of the 840W proto-type LCR-DAB converter.

## Feature of the LCR-DAB converter

Figure 1 shows the SST applied to the MV (Medium Voltage)/LV (Low Voltage) system that converts the distribution system voltage of 22.9[kV] to 220[V]. If this system is designed to have an electrical breakdown voltage of 1.5 times the grid voltage, an electrical breakdown voltage of 35[kV] or higher is required. Since the high-frequency transformer of the conventional DAB converter has a relatively small volume, however, it is difficult to secure the high insulation performance required for a higher breakdown voltage than 35[kV]. Figure 2 depicts the proto-type LCR-Coil of the LCR-DAB converter used in this paper. As shown in the figure, the distance between the two WPT coils in the LCR-Coil designed in this paper is 3[cm]. If the material inside the distance is air, the electrical breakdown voltage between the primary and secondary coils of the LCR-coil is approximately 60[kV]. Therefore, in case an LCR-DAB converter is used instead of a high-frequency transformer of the conventional DAB converter, high insulation performance can be easily secured. Figure 3 shows the configuration of the LCR-DAB converter. As shown in the figure, The LCR-DAB converter is configured with the additional compensation circuit for efficient power transfer, such as the general Wireless Power Transmission (WPT) system. The compensation circuit is generally composed of a resonant circuit using capacitors, and the LCR-DAB converter in figure 3 is the Series-Series (SS) compensation circuit with the capacitor in series in the coil. The SS compensation circuit is one of the compensation circuits mainly used in the WPT system because it has the characteristics of the voltage source or the current source depending on the operating frequency of the converter [10]. Therefore, in this paper, the SS compensation circuit was applied as a method to compensate for the coupling coefficient.

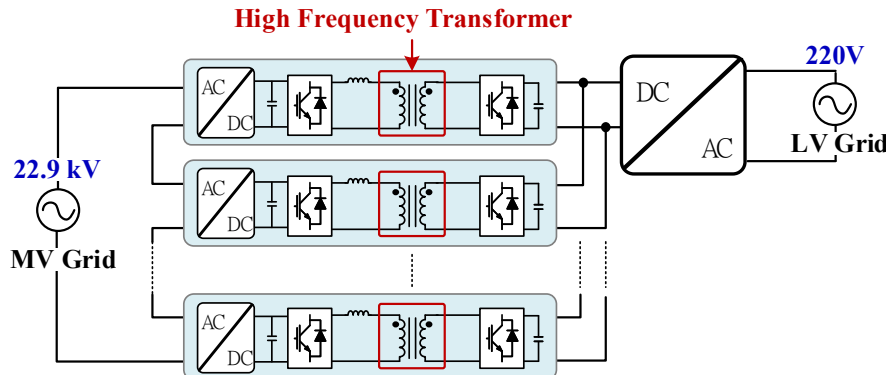


Fig. 1: SST applied to MV/LV system

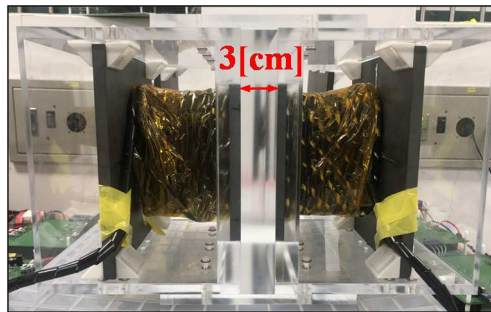


Fig. 2: LCR-coil applied to 840[W] class LCR-DAB converter

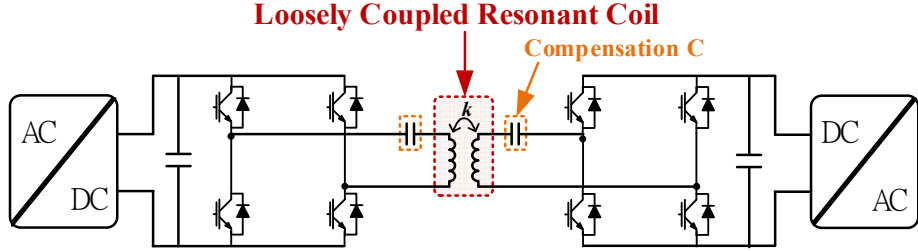


Fig. 3: Configuration of the LCR-DAB converter

**Table I: Parameters of the proto-type LCR-DAB converter**

Parameters	Value
$V_P, V_S$ (Priamry & secondary DC voltage)	100 [V]
$C_P, C_S$ (Series capacitance)	72 [nF]
$R_P, R_S$ (Coil resistance)	70 [mΩ]
$L_P, L_S$ (Series inductance)	100 [uH]
$k$ (Coupling coefficient)	0.26

## Impedance characteristics of the LCR-DAB Converter with SS compensation circuit

The conventional DAB converter having a high-frequency transformer can transfer power between primary and secondary converters by phase angle difference of the primary and secondary output voltages. Because the power transferred can be simply determined by the phase angle difference namely phase-shift, the power can be controlled easily. In a similar manner, the power control of the LCR-DAB converter can be performed through phase-shift of the secondary converter output voltage at the fixed operating frequency. However, the electric circuit characteristics of the WPT coils and the series capacitor in the LCR-DAB converter change according to the phase-shift. Therefore, to determine the operating frequency of the LCR-DAB converter, it is necessary to analyze the characteristics of the input impedance according to the phase shift. In the case of LCR-DAB converters which are consisted of the WPT coils and series capacitors, the input impedances have three resonant frequencies. Each resonance frequency can be calculated through Short/Open circuit analysis from the equivalent circuit of the LCR-DAB converter [5]. Figure 4 shows the equivalent circuit of the LCR-DAB converter. Both wireless coils of the LCR-DAB converter can be equivalent to T-model for electrical analysis as shown in the figure 4. In figure 4,  $V_P, V_S$  are converter output voltages,  $\theta$  is phase-shift angle of  $V_S$  relative to  $V_P$ ,  $I_P, I_S$  are converter currents,  $R_P, R_S$  are Equivalent Series-Resistances (ESR) of the wire,  $C_P, C_S$  are capacitances of compensation capacitors,  $L_P, L_S$  are self-inductances, and  $k$  is coupling coefficient between the primary coil and the secondary coil, respectively.

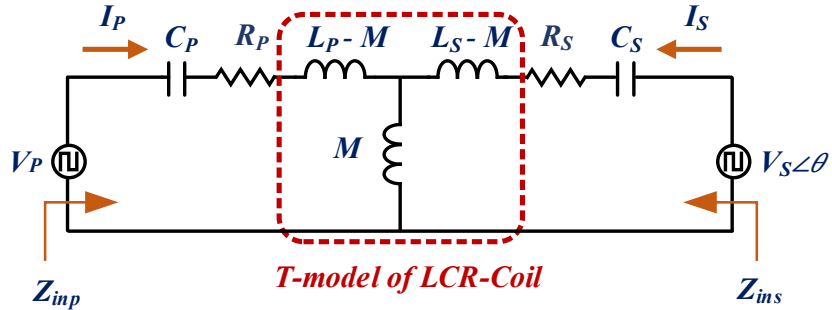


Fig. 4: The equivalent circuit of the LCR-DAB converter

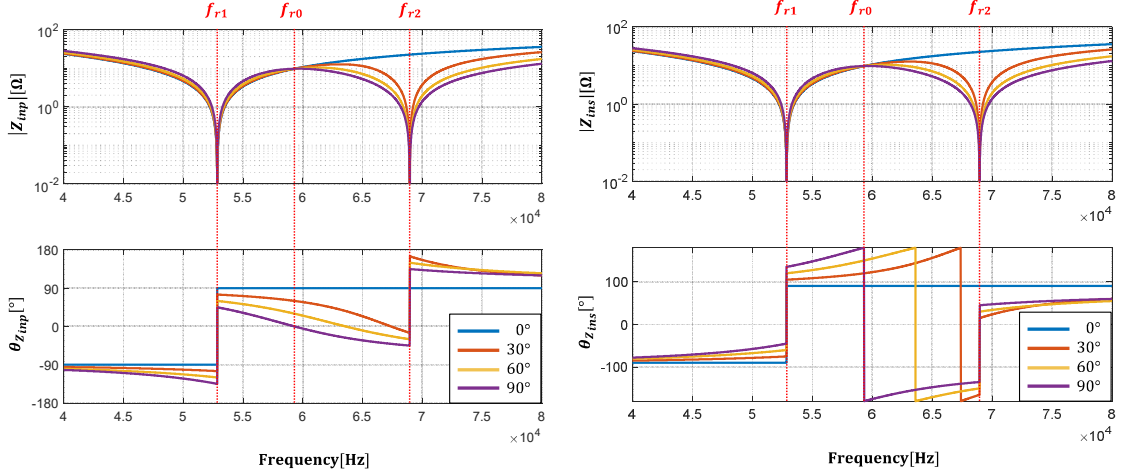


Fig. 5: Frequency responses of input impedances by phase-shift

In addition,  $Z_{inp}$  and  $Z_{ins}$  represent the input impedance seen from primary converter and secondary converter, respectively. From figure 4, if  $L_P=L_S$ ,  $C_P=C_S$ , and  $R_P=R_S=0[\Omega]$ , each resonant frequency of input impedances can be expressed as the following equations.

$$f_{r0} = \frac{1}{2\pi\sqrt{L_P C_P}} = \frac{1}{2\pi\sqrt{L_S C_S}} \quad (1)$$

$$f_{r1}, f_{r2} \cong \frac{f_{r0}}{\sqrt{1 \pm k}} \quad (2)$$

In equations (1) and (2),  $f_{r0}$  is the series resonance frequency of the short circuit in the LCR-DAB converter equivalent circuit, and  $f_{r1}, f_{r2}$  are the two resonance frequencies of the open circuit. Figure 5 shows the frequency response characteristics of the input impedance according to the phase-shift. The specifications in table 1 were applied to the input impedance calculations. Figure. 5 indicates that the Q at  $f_{r1}$  decreases and the Q at  $f_{r2}$  increases as the phase-shift increases. Therefore, in the frequency band between  $f_{r1}$  and  $f_{r0}$ , the input impedance increases as the phase-shift increases, and in the frequency band between  $f_{r0}$  and  $f_{r2}$ , the input impedance decreases as the phase-shift increases. On the other hand, at the series resonance frequency  $f_{r0}$ , the input impedance magnitude is always constant regardless of the phase-shift.

## Selection of operating frequency of LCR-DAB converter to apply fixed frequency PSM

The proposed power control method of the LCR-DAB converter would control the transferred power through only phase-shift. Therefore, because the switching frequency needs to be fixed for the simplicity of the control structure, the switching frequency should be determined from the viewpoint of efficiency. In figure 5, in the frequency band between  $f_{r1}$  and  $f_{r0}$ , it was confirmed that the magnitude of the input impedances increased as the phase-shift increases. However, since the input impedance in this frequency band is relatively small, the magnitude of the average current in the phase-shift range ( $-90[^\circ]$ ~ $90[^\circ]$ ) is large. Figure 6 shows the average input current according to the phase-shift range in case the LCR-DAB converter is operated with a frequency between  $f_{r1}$  and  $f_{r0}$ . In the figure, it can be confirmed that the case of  $f_{r0}$  has the lowest average input current in the entire phase-shift range. On the other hand, in the frequency band between  $f_{r0}$  and  $f_{r2}$ , as the phase shift increases, the magnitude of the input impedance decreases. Therefore, in this frequency band, the magnitude of the input current increases as the phase shift increases. In addition, in this frequency band, as the phase shift increases, the decrease in input impedance is relatively large. Therefore, even when the phase shift is less than  $90^\circ$ , the impedance phase becomes  $0^\circ$ . This means that when the LCR-DAB converter operates at a frequency higher than  $f_{r0}$ , the rated power is output even when the phase shift is less than  $90^\circ$ . Consequently, when the LCR-DAB converter operates at a frequency

between  $f_{r0}$  to  $f_{r2}$ , the usable range of the phase shift, which is the only control variable, is reduced, thereby increasing the control sensitivity. Figure 7 shows the output power for the phase shift in the case of the LCR-DAB converter operated at a frequency between  $f_{r0}$  and  $f_{r0}-f_{r2}$ (65kHz). In the case of  $f_{r0}$  in the figure, the output power increases according to the phase-shift, and the rated power is output under the condition that the phase-shift is  $90^\circ$ . On the other hand, at a frequency between  $f_{r0}$  and  $f_{r2}$ (65kHz), the rated power can be transferred at the phase-shift of about  $40^\circ$ , and as the phase-shift increases, the transferred power would be larger than the rated power. When the LCR-DAB converter operates at  $f_{r0}$  with the PSM method, the magnitude of input current is minimized as compared with other frequencies, and the range of phase-shift angle capable of transmitting rated power is extended to  $90^\circ$ , thereby minimizing control sensitivity. In addition, the magnitude of input impedance is constant, and the input impedance have inductive characteristics in the entire phase-shift range. Therefore, the current magnitude would not only be constant in the whole power range, but the ZVS operation is also achieved in the whole power range.

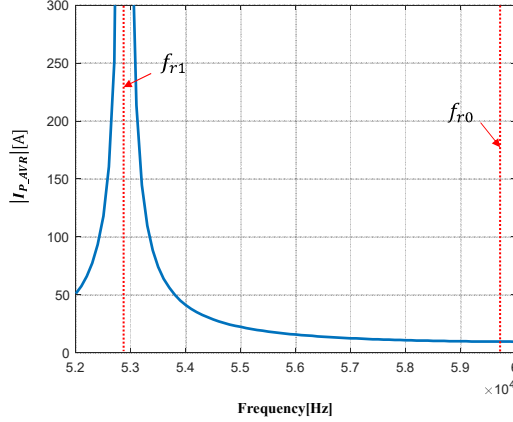


Fig. 6: Average input current magnitude for frequencies between  $f_{r1}$  and  $f_{r0}$

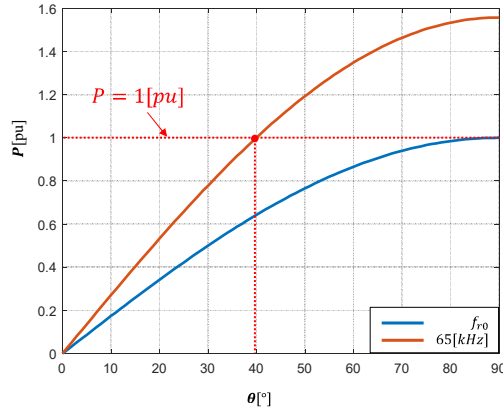


Fig. 7: Output power for phase-shift in case of  $f_{r1}$  and 65kHz

### Proposed power control of LCR-DAB converter with fixed frequency PSM

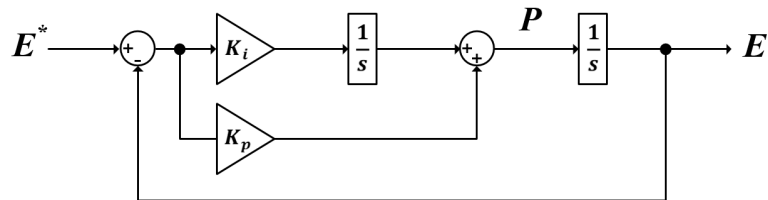


Fig. 8: Power controller structure

Typically, the conventional DAB converter controls the amount of power flowing through the converter to control the secondary DC-link voltage [11]. Figure 8 shows the structure of the voltage controller applied in this paper, and the energy, which is the input variable of the power controller, was calculated from the DC-link voltage using the following equation:

$$E = \frac{1}{2}CV^2 \quad (3)$$

The reference value is the stored energy when the secondary DC link capacitor voltage is the command voltage ( $V_{DCS}^*$ ) and the feedback value is the stored energy in the secondary DC link capacitor of which value is  $V_{DCS}$ . In equation (3),  $C$  is the capacitances of DC-link. To apply PSM to the control structure shown in Fig. 8, an operator is required to convert power, which is the output of the power controller, into the phase-shift. Therefore, it is necessary to derive a power equation having the phase-shift as a variable. The power equation of the LCR-DAB converter can be derived by analyzing the LCR-DAB converter equivalent circuit in Figure 4. From the equivalent circuit of the LCR-DAB converter, assuming that  $L_P=L_S$ ,  $C_P=C_S$ , and  $ESR=0[\Omega]$ , the power equation of the LCR-DAB converter operating at  $f_{r0}$  can be simply expressed as follows:

$$P_P = -\frac{1}{2}Re\{V_P I_P\} \cong -\frac{V_P^2}{Z_{inpo}} = -\frac{V_P V_S}{2\omega_{r0}M} \sin\theta \quad (4)$$

$$P_S = -\frac{1}{2}Re\{V_S I_S\} \cong -\frac{V_S^2}{Z_{ins0}} = \frac{V_P V_S}{2\omega_{r0}M} \sin\theta \quad (5)$$

In equations (4) and (5),  $Z_{inpo}$  and  $Z_{ins0}$  are the input impedance when the LCR-DAB converter operates at  $f_{r0}$ ,  $\omega_{r0}$  ( $= 2\pi f_{r0}$ ) is the angular frequency, and  $M$  ( $= k\sqrt{L_p L_s}$ ) is the mutual inductance, respectively. From the derived power equation, it can be seen that the sign of the power and the sign of the phase-shift are opposite in the LCR-DAB converter, unlike the conventional DAB converter. Therefore, in the case of an LCR-DAB converter, when power is transferred from the primary side to the secondary side, the output voltage of the primary side converter is led the output voltage of the secondary side converter, and in the opposite case, the primary side output voltage is lagged than the secondary side output voltage. From Equations (4) and (5), assuming that the magnitude of the phase-shift is small, the operator for deriving the phase-shift from the output of the power controller can be expressed as follows.

$$\theta_P = -\frac{2\omega_{r0}M}{V_P V_S} P_P \quad (\text{Power flow } P \rightarrow S) \quad (6)$$

$$\theta_S = \frac{2\omega_{r0}M}{V_P V_S} P_S \quad (\text{Power flow } S \rightarrow P) \quad (7)$$

Figure 9 shows the power control structure of the LCR-DAB converter proposed in this paper. Figure 9 shows the control structure when power is transmitted from the primary side to the secondary side, and Equation (6) is applied to calculate the phase-shift. On the other hand, when power is transmitted from the secondary side to the primary side, power control can be performed by calculating the phase-shift using Equation (7)

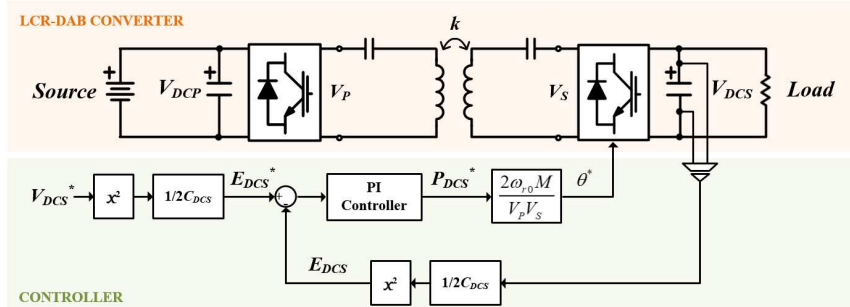


Fig. 9: Proposed power controller structure of the LCR-DAB converter

## Results of experiment

To verify the proposed power controller of the LCR-DAB converter, the 840[W] proto-type LCR-DAB converter power control experiments were performed. Figure 10 shows the experiment set-up, and the specifications of the system used for the experiment are described in Table 1. Figure 11 shows the voltage and current waveforms when there is no load and when the rated load is applied in each direction. In Figure 11, as confirmed by Equations (4) and (5), since the sign of power and the sign of phase are opposite, it can be confirmed that the phase-shift increases in the opposite direction as the load increases. In addition, since the magnitude of the input impedance is constant regardless of the phase-shift in case of operating at the series resonance frequency ( $f_{r0,i}$ ), it can be confirmed that the magnitude of the input current is almost constant under all load conditions. Figure 12 shows the load current and the secondary DC link voltage when the rated load is applied in the stepped manner. In figure 12, it can confirm that the DC link voltage is well controlled even with a momentary load change. Figure 13 shows the efficiency and input-output loss for the output power of the LCR-DAB converter. The maximum efficiency is about 96.8[%] was measured when power is transmitted from the secondary side to the primary side, and the loss was measured in the form of a decrease as the load increased. Since the LCR-DAB converter performs the ZVS operation in all load conditions, the loss of the converter is dominated by the resistance loss due to the converter current. Therefore, ideally, since the magnitude of the converter output current is constant regardless of the load when operating at the series resonance frequency, a constant loss should occur even when the load changes. However, due to the error of the system parameter, the current increased as the load increased, and the loss was measured in the form of a decrease.

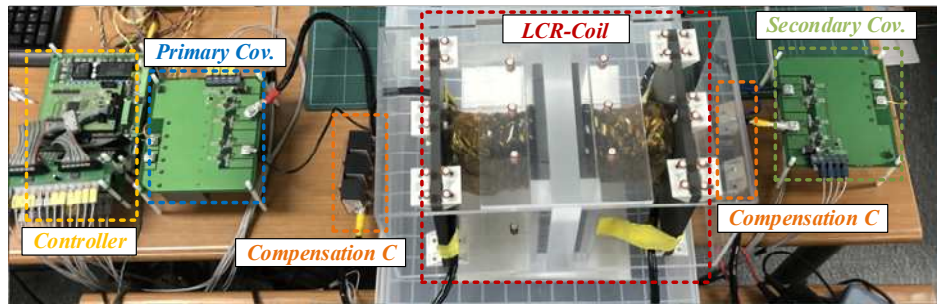


Fig. 10: Experiment set-up of 840W LCR-DAB converter

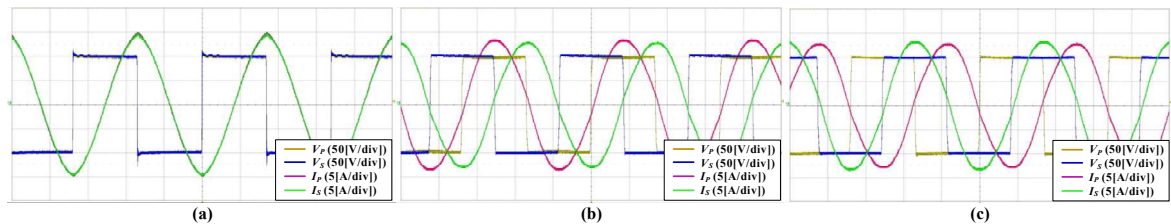


Fig. 11: (a) No-load, (b) Rated load (positive direction), (c) Rated load (negative direction)

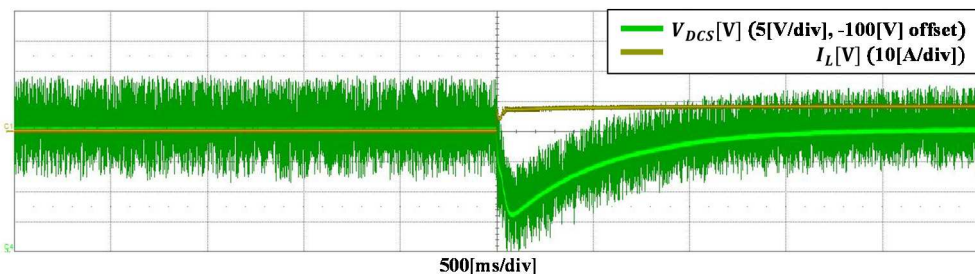


Fig. 12: The load current and the secondary side DC link voltage for the step rated load

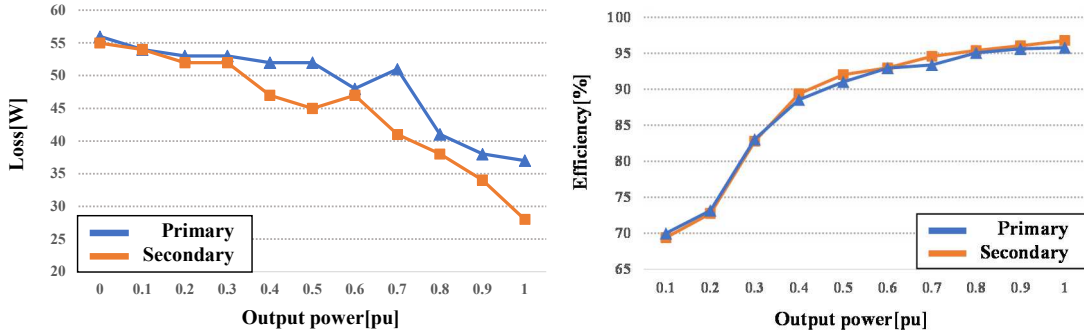


Fig. 13: Efficiency and loss for output power

## Conclusion

In this paper, the power control method of applying the fixed frequency PSM that can perform with a relatively simple structure to the LCR-DAB converter was proposed. To this end, the selection of the most suitable compensation topology and efficient switching frequency for the LCR-DAB converter was described. The validity of the proposal was verified through the power control experiment of the 840[W] proto-type LCR-DAB converter to which the selected efficient frequency was applied.

## References

- [1] J. E. Huber and J. W. Kolar: Applicability of Solid-State Transformers in Today's and Future Distribution Grids, IEEE Transactions on Smart Grid, vol. 10, no. 1, pp. 317- 326
- [2] R. P. Londero, A. P. C. d. Mello and G. S. da Silva: Comparison between conventional and solid state transformers in smart distribution grids, IEEE PES Innovative Smart Grid Technologies Conference, pp. 1- 6
- [3] A. Joshi and S. Nath: Efficiency Comparison of Solid-State Transformer and Low-Frequency Power Transformer, 3rd International Conference on Energy, Power and Environment: Towards Clean Energy Technologies, pp. 1- 6
- [4] B. Zhao, Q. Song, W. Liu, and Y. Sun: Overview of dual-active-bridge isolated bidirectional DC-DC converter for high-frequency-link power-conversion system, IEEE Transactions on Power Electronics, vol. 29, no. 8, pp. 4091- 4106
- [5] X. She, A. Q. Huang and R. Burgos: Review of Solid-State Transformer Technologies and Their Application in Power Distribution Systems, IEEE Journal of Emerging and Selected Topics in Power Electronics, vol. 1, no. 3, pp. 186- 198
- [6] J. E. Huber and J. W. Kolar: Solid-State Transformers: On the Origins and Evolution of Key Concepts, IEEE Industrial Electronics Magazine, vol. 10, no. 3, pp. 19- 28
- [7] J. E. Huber and J. W. Kolar: Volume/weight/cost comparison of a 1MVA 10 kV/400 V solid-state against a conventional low-frequency distribution transformer, 2014 IEEE ECCE, pp. 4545- 4552
- [8] J. Lee, J. Roh, S. -H. Lee, S. Kim and M. -Y. Kim: A Novel Solid-State Transformer with Loosely Coupled Resonant Dual-Active-Bridge Converters, in 2020 IEEE ECCE, pp. 3972- 3978
- [9] J. Lee, J. Roh, M. Y. Kim, S. -H. Baek, S. Kim and S. -H. Lee: A Novel Solid-State Transformer With Loosely Coupled Resonant Dual-Active-Bridge Converters, IEEE Transactions on Industry Applications, vol. 58, no. 1, pp. 709- 719
- [10] S. Cho, I. Lee, S. Moon, G. Moon, B. Kim and K. Y. Kim: Series-series compensated wireless power transfer at two different resonant frequencies, IEEE ECCE Asia Downunder, pp. 1052- 1058
- [11] C. Mi, H. Bai, C. Wang, S. Gargies: Operation, Design and Control of Dual H-bridge-based Isolated Bidirectional DC-DC Converter, IET Power Electronics, vol. 1, no. 4, pp. 507- 517